Cell Calcium 71 (2018) 75–85

Contents lists available at ScienceDirect

Cell Calcium

journal homepage: www.elsevier.com/locate/ceca

Anoctamin 9/TMEM16J is a cation channel activated by cAMP/PKA signal

Hyungsup Kim[a,b], Hyesu Kim[a,b], Jesun Lee[a], Byeongjun Lee[b], Hee-Ryang Kim[a], Jooyoung Jung[b], Mi-Ock Lee[a,**], Uhtaek Oh[a,b,*]

[a] College of Pharmacy, Seoul National University, Seoul, 08826, Republic of Korea
[b] Brain Science Institute, Korea Institute of Science and Technology (KIST), Seoul, 02792, Republic of Korea

ARTICLE INFO

Keywords:
Anoctamins
PKA
cAMP
Cation channel
Calcium

ABSTRACT

Anoctamins (ANOs) are multifunctional membrane proteins that consist of 10 homologs. ANO1 (TMEM16A) and ANO2 (TMEM16B) are anion channels activated by intracellular calcium that meditate numerous physiological functions. ANO6 is a scramblase that redistributes phospholipids across the cell membrane. The other homologs are not well characterized. We found ANO9/TMEM16J is a cation channel activated by a cAMP-dependent protein kinase A (PKA). Intracellular cAMP-activated robust currents in whole cells expressing ANO9, which were inhibited by a PKA blocker. A cholera toxin that persistently stimulated adenylate cyclase activated ANO9 as did the application of PKA. The cAMP-induced ANO9 currents were permeable to cations. The cAMP-dependent ANO9 currents were augmented by intracellular Ca^{2+}. *Ano9* transcripts were predominant in the intestines. Human intestinal SW480 cells expressed high levels of *Ano9* transcripts and showed PKA inhibitor-reversible cAMP-dependent currents. We conclude that ANO9 is a cation channel activated by a cAMP/PKA pathway and could play a role in intestine function.

1. Introduction

The Anoctamin/TMEM16 family consists of transmembrane proteins in 10 isoforms, ranging from ANO1/TMEM16A to ANO10/TMEM16K. Anoctamins are expressed in numerous major tissues and are thought to mediate various physiological functions. The best-known anoctamin gene is *Ano1*, which is a Cl^- channel activated by Ca^{2+} [1–3]. ANO1 is known to mediate transepithelial fluid movements such as salivation in the salivary glands, mucin secretion in the airway and Cl^- and fluid secretion in the intestine [4–8]. ANO1 is also highly expressed in small-diameter dorsal-root ganglion neurons, implicating its role in nociception as a heat sensor [9]. Also, ANO1 plays an important role in controlling smooth muscle contraction [10] and pacemaking activity in the intestine [11,12]. More importantly, ANO1 is implicated in tumorigenesis [13–15] and benign prostate hyperplasia [16].

ANO2 is a Cl^- channel activated by Ca^{2+} and is thus also considered a Ca^{2+}-activated Cl^- channel [4,17]. ANO2 has physiological functions distinct from ANO1; it controls sensory transduction and synaptic plasticity in the central nervous system [18,19] as well as olfactory transduction and phototransduction [20–24]. Also, ANO2 is involved in smooth muscle contraction [25,26].

Unlike ANO1 and ANO2, ANO6/TMEM16F has dual functions. ANO6 is a small conductance calcium-activated cation channel (SCAM) that is permeable to divalent ions [27]. Strikingly, ANO6 is known to be a scramblase that disrupts polarized phospholipids in the plasma membrane. The polarized phospholipids attract immunological signals necessary for activation of T lymphocytes [28–30]. Mutations in *Ano6* cause a rare bleeding disease, Scott syndrome [31,32]. Thus, ANO6 is both a channel and an enzyme. Some scramblase activity has also been observed in ANO4, ANO8 and ANO9 [33].

ANO5 is involved in skeletomuscular function; its mutations cause gnathodiaphyseal dysplasia, an autosomal dominant inherited bone disorder [34]. However, its biophysical properties and mechanism of activation are unknown.

Although the functional roles of some genes in the Anoctamin family are well studied, the role of ANO9/TMEM16J remains poorly understood [35]. ANO9 is found in the human nasal and colonic epithelium and expressed in the respiratory, digestive, skeletal and integumentary systems during development [36]. ANO9 is also implicated in the metastasis of colorectal cancer [37]. In a recent study, ectopic expression of ANO9 in the pancreas is associated with poor prognostic pancreatic cancer [38]. Despite its expression pattern and a possible role in tumorigenesis, the function and activation mechanism of ANO9 is not known. The present study aimed to determine if ANO9 is a channel and, if so, how it is activated. Surprisingly, we found that ANO9 is a cation channel activated by the cAMP/PKA pathway.

* Corresponding author at: Brain Science Institute, Korea Institute of Science and Technology (KIST) 5, Hwarang-ro, 14-gil, Seongbuk-gu, Seoul, 02792, Republic of Korea.
** Corresponding author at: College of Pharmacy 20-418, Seoul National University, 1 Gwanak-ro, Gwanak-gu, Seoul, 08826, Republic of Korea.
E-mail addresses: molee@snu.ac.kr (M.-O. Lee), utoh@kist.re.kr (U. Oh).

https://doi.org/10.1016/j.ceca.2017.12.003
Received 10 October 2017; Received in revised form 16 December 2017; Accepted 26 December 2017
Available online 30 December 2017
0143-4160/

2. Material and methods

2.1. Cloning of mouse Ano9 and mutagenesis

Primers were designed using the mouse cDNA sequences of *Ano9* (TMEM16J) from the NCBI database (NM_178381.3). The cDNA encoding *Ano9* has been isolated from the lung of adult C57BL/6J mice. The full-length coding sequence of *Ano9* (Tmem16J; NM_178381.3) was amplified by PCR using site-specific primers:

forward primer 5′- GCCACCATGCAGGATGATGAGAGTTCCCAG-3′, reverse primer 5′- GACCGGTCTATACATCCGTGCTCCTGGAAC-3′.

Ano9 were cloned into pEGFP-N1 to have fusion proteins tagged with EGFP. To express ANO9–GFP fusion protein, a stop codon was deleted from pEGFP-N1-mANO1 using the Muta-Direct site-directed mutagenesis kit (iNtRON Biotech). The protein sequence of mouse *Ano9* (NP_848468.2) is

MQDDESSQIFMGPEGDQLPLVEMGSCKPEASDQWDCVLVADLQTLKIQK
HAQKQLQFLENLESNGFHFKMLKDQKKVFFGIRADSDVIDKYRTLLMNP
EDSGSRDEQSFNIATTRIRIVSFVVNNKLKPGDTFEDLVKDGVFETMFLLH
KGEQNLKNIWARWRNMFEPQPIDEIREYFGEKVALYFTWLGWYTYMLV
PAAVVGLIVFLSGFALFDSSQISKEICSANDIFMCPLGDHSHRYLRLSEMCT
FAKLTHLFDNEGTVLFAIFMALWATVFLEIWKRKRAHEVQSWKLYEWDE
EEEEMALELINSPHYKLKDHRHSYLSSTIILILSLFMICLMIGMAHVLVVYR
VLAGALFSSLVKQQVTTAVVVTGAVVHYIIIVIMTKVNKYVALKLCKFEES
GTFSEQERKFTVKFFILQFFAHFSSLIYIAFILGRINGHPGKSTRLAGLWKLE
ECHLSGCMMDLFIQMAIIMGLKQTLSNCVEYLCPLLAHKWRLMWASKH
GHMSKDPELKEWQRNYYMNPINTFSLFDEFMEMMIQYGFTTIFVAAFPL
APLLALFSNLVEIRLDAIKMVRLQRRLVPRKAKDIGTWLQVLETIGVLAVI
ANGMVIAFTSEFIPRVVYKYHYGPCRTNRTFTDDCLTNYVNHSLSVFYTK
HFNDHSRMEGQENVTVCRYRDYRNEHDYNLSEQFWFILAIRLTFVILFEH
FALCIKLIAAWFVPDVPQKVKNEVLQEKYDRIRHRMRFSSRSTDV.

Haemagglutinin (HA) epitope (YPYDVPDYA) was added to the N-terminus of *mAno9* using the HA-pcDNA3.1 vector to generate HA-tagged *mAno9* mutants.–>

2.2. Cell culture and transfection of Ano9

Cell culture and functional expression of ANO9 or HA-ANO9 were performed in HEK293T cells. HEK293T cells were maintained at 5% CO_2, and incubated at 37 °C in Dulbecco's modified Eagle's medium (DMEM) supplemented with 10% fetal bovine serum (FBS), 10 units/mL penicillin and 10 μg/mL streptomycin. To induce ANO9 expression in HEK293T cells, cells were transfected with *mAno9* cDNA mixed with the FuGene HD (Roche Diagnostics) transfection reagent. The transfected cells were plated onto glass coverslips. The current responses were recorded 24–48 h after transfection.

2.3. Whole-cell and single-channel current recordings

Whole-cell and single-channel current recordings were obtained using either a voltage-clamp technique with an Axopatch 200B amplifier (Molecular Devices) as descried previously [9,39]. Briefly, whole-cell currents were measured after breaking the plasma membrane under the pipette tips. The resistance of the glass pipettes was about 3 mΩ. The junctional potentials were cancelled to zero. Unless otherwise stated, the bath solution contained (in mM) 140 NaCl, 2 $CaCl_2$, 2 $MgCl_2$ and 10 NaOH-HEPES adjusted to pH 7.2. The pipette solution contained (in mM) 140 KCl, 2 $CaCl_2$, 2 $MgCl_2$ and 10 KOH-HEPES adjusted to pH 7.2. The osmolarity of the pipette and bath solutions was adjusted to 300 mOsm/L by adding mannitol.

For inside-out patch recording, after a giga-seal was formed, the glass pipette was pulled quickly from the cell to isolate a membrane patch. The output of the amplifier was fed to an analog/digital converter (Digidata 1440, Molecular Devices) and stored in a personal computer. The pClamp 10 software was used for I–V curve and other biophysical analysis.

Ca^{2+} was chelated with 10 mM EGTA and 10 mM HEDTA to make the free 1.0 and 10 μM Ca^{2+} in the pipette solutions, respectively. The free Ca^{2+} was calculated using WEBMAXC (http://www.stanford.edu/~cpatton/webmaxcS.htm).

2.4. Immunofluorescent staining

SW480 cells were fixed on glass coverslips in 4% paraformaldehyde for 10 min at room temperature, permeabilized with 0.2% Triton X-100, and incubated with anti-ANO9 antibodies (dilution 1:200, LS-C179041, LifeSpan BioSciences, Inc.) overnight at 4 °C. The coverslips were washed and incubated with the Alexa Fluor 488-tagged donkey-anti-rabbit IgG (1:1000, Molecular Probes, CA). For nuclear staining, SW480 cells and HEK293T cells were incubated with Hoechst 33342 (H3570, Thermofisher Scientific, 1:2000) after ANO9 immunostaining.

2.5. Small interfering RNA (siRNA) treatment

Two nucleotide oligomer siRNAs targeting human *Ano9* or scrambled siRNA labelled with Cy3 were provided by Bioneer (Seoul, Korea) transfected into cells using Lipofectamine 2000™ (Invitrogen) 1 day after plating. We transfected the cells with a mixture of the two siRNAs simultaneously for maximal effect. The two siRNAs (Nos. 1152997 and 1152999) are as follows.

1152997 Sense: GUGAACUUCGUUGUCAUGA(dTdT), 1152997 Antisense: UCAUGACAACGAAGUUCAC(dTdT),

1152999 Sense: UCAGCAACUGCGUCGAGUA(dTdT), 1152999 Antisense: UACUCGACGCAGUUGCUGA(dTdT).

2.6. Calcium imaging

ANO9-HEK cells or mock-HEK cells were loaded with Fluo3-AM (Invitrogen) containing 0.1% Pluronic F-127 (Invitrogen). After loading with Fluo3-AM for 40 min, db-cAMP alone or with H-89 was applied to the cells. The fluorescence intensities of cells were measured at 488 nm in every 5 s with a confocal microscope (LSM700, Zeiss).

2.7. Real-time quantitative PCR

Major mouse organs were isolated from three 7-week-old mice. The total RNAs from each organ were purified with ethanol precipitation or the Easy Spin™ Total RNA Extraction Kit (iNtROn Biotech) according to the manufacturer's protocol. The first strand cDNAs were reverse transcribed from the total RNA using the Transcriptor First Strand cDNA Synthesis Kit (Roche). To measure the gene expression level, we performed real-time quantitative PCR (qPCR) in the LightCycler 2.0 system (Roche) using an ANO9 specific universal probe (forward primer: cggactctcctcatgaatcc; reverse primer: tgttcacgacaaagctcaca). The absolute copy numbers per 250 ng of total RNA were calculated using the absolute quantification with the external standard method in the Light Cycler software 4.0.

2.8. Immunoprecipitation and in vitro PKA assay

For the immunoprecipitation assay, HEK293T cells were transfected with the HA-*Ano9* plasmids. The transfected HEK cells were washed with ice-cold phosphate buffered saline. The cells were harvested with RIPA buffer supplemented with a protease inhibitor cocktail (cOmplete™, Roche) and a phosphatase inhibitor cocktail (Sigma, P0044). The cells were lysed with repeated vortexing for 30 min. The cell lysates were mixed with anti-HA antibodies (Sigma, H6908) or anti-ANO9 antibodies (Lifespan Bioscience, C179041) and incubated overnight in 4 °C. The immune complexes were collected after binding to protein A beads (Sigma, P3476) and washed twice with 1X kinase buffer. Pellets were suspended in 40 μl 1X kinase buffer supplemented

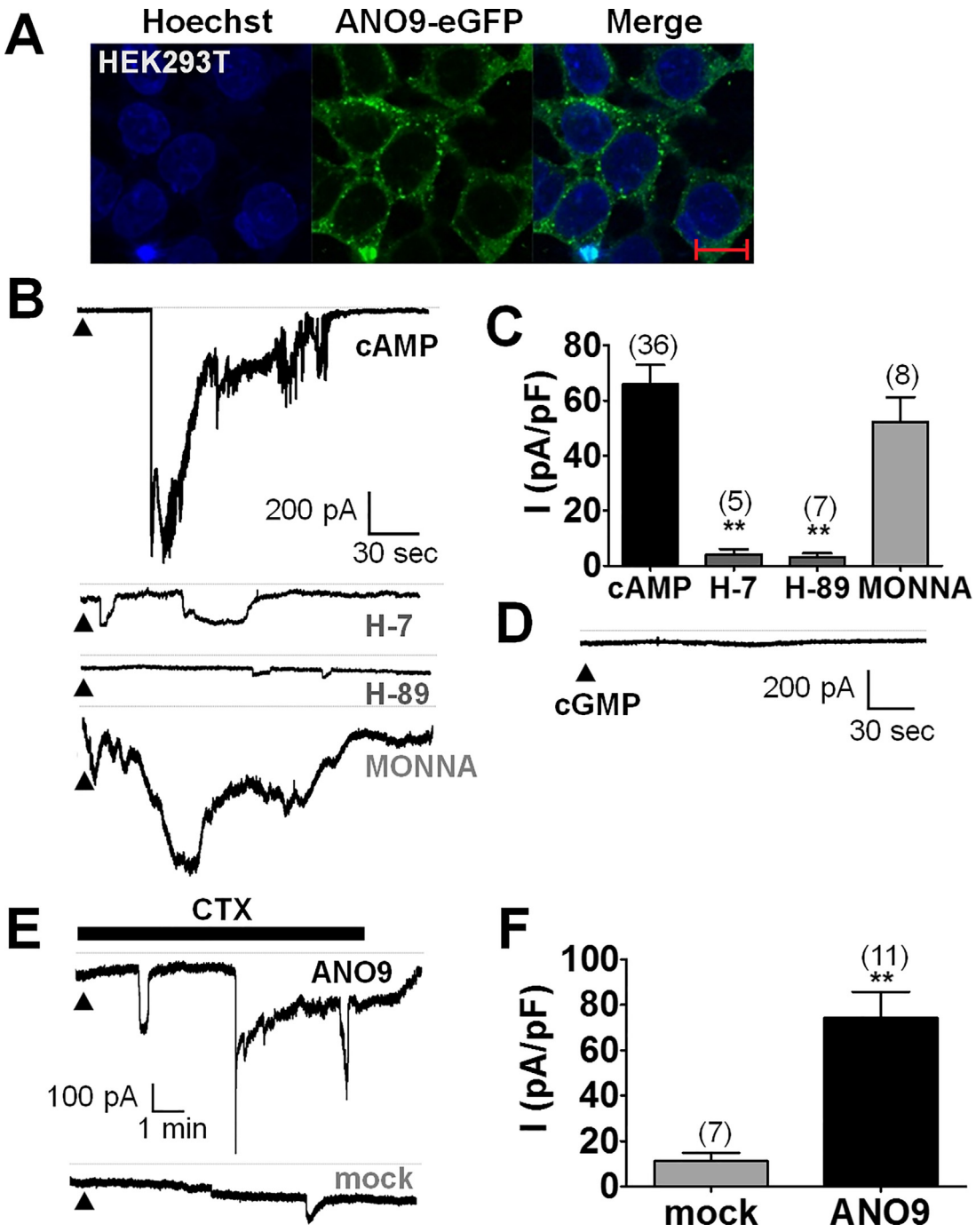

Fig. 1. Intracellular cAMP activates ANO9.

(A) The overexpression of mANO9-pEGFP-N1 in the HEK293T cells with Hoechst 33342 staining (left).

(B) Representative traces of whole-cell currents of HEK293T cells transfected with Ano9. The bath solution contained (in mM) 140 NaCl, 2 $MgCl_2$ and 2 $CaCl_2$ buffered with 10 HEPES, and the pipette solution contained 140 KCl, 2 $MgCl_2$, 2 ATP, 0.3 GTP buffered with 10 mM HEPES. cAMP (100 μM) was added to the pipette solution. $E_{hold} = -60$ mV. Note that intracellular cAMP evoked robust inward currents in the ANO9-HEK cells but not in the H-7 and H-89 pre-treated cells. The treatment of an ANO1-antagonist, MONNA, failed to block the cAMP-induced ANO9 current. The dashed lines represent zero current. Arrow head represents the time for forming a whole cell.

(C) Summary of the cAMP-induced whole-cell currents of control (cAMP) and the H-7, H-89, MONNA pre-treated ANO9-HEK cells. The error bars represent S.E.M. ** $p < 0.01$, one way ANOVA followed by Tukey's post-hoc test. Numbers in parenthesis represent the experimental numbers.

(D) A representative trace of whole-cell currents of ANO9-HEK cells with 100 μM cGMP in the pipette solution.

(E) The cholera toxin (CTX) applied to the bath evoked whole-cell inward currents in ANO9-HEK cells but not in mock-transfected HEK293T cells.

(F) Summary of the CTX-induced currents in ANO9-HEK cells.

with 200 μM ATP and recombinant catalytic subunit of PKA (New England Biolabs, P6000S). Suspended lysates were incubated 30 min at 30 °C. The samples were heated at 95 °C for 5 min with 2X SDS sample buffer. The samples in SDS buffer were separated by SDS–PAGE. The separated proteins were transferred to a PVDF membrane that was incubated with the appropriate primary and secondary antibodies. Protein bands were detected by chemiluminescent substrates (Thermo Scientific, 34095). The immunoprecipitates and lysates were immunoblotted with anti-phosphoserine antibodies (Sigma, P5747), anti-HA antibodies, or anti-ANO9 antibodies.

2.9. Reagents

We purchased adenosine 3′,5′-cyclic monophosphate (cAMP; A9501), Cholera toxin from *Vibrio cholera* (CTX; C8052), N6,2′-*O*-dibutyryladenosine 3′,5′-cyclic monophosphate (db-cAMP) sodium salt (D0627), protein kinase A from bovine heart (PKA; P5511), H-89 dihydrochloride hydrate (B1427), H-7 dihydrochloride (I7016) and 4-aminopyridine (275875) from Sigma-Aldrich.

All basic chemicals for the electrophysiology experiments were also purchased from Sigma-Aldrich.

2.10. Statistical analysis

All results are expressed as means ± standard errors (S.E.). The statistical significances of the differences were determined by a one-way analysis of variance (ANOVA) followed by the Tukey's post-hoc test for multiple comparisons. Statistical significance was accepted at p values of less than 0.05.

3. Results

3.1. cAMP activates ANO9

To determine if ANO9 is a channel, we expressed mouse ANO9 tagged on the C terminus with enhanced green fluorescence protein (eGFP) for visual identification in HEK293T cells. The eGFP was largely localized in the plasma membrane (Fig. 1A). Upon whole-cell formation in the HEK293T cells transfected with *Ano9-eGFP* (ANO9-HEK cells), robust inward currents (65.9 ± 6.99 pA/pF, n = 36) were observed with E_{hold} = −60 mV when the pipette solution contained 100 μM cAMP. The bath and pipette solutions contained 140 mM NaCl and 140 mM KCl, respectively. These currents were not observed in whole cells without cAMP in the pipette. Also, the cAMP-evoked currents were completely blocked by the treatment of the cells with PKA blockers (20 μM H-7 or 20 μM H-89; Fig. 1B and C). cGMP in the pipettes (100 μM) failed to evoke currents in ANO9-HEK cells (Fig. 1D). The cAMP-evoked currents in the ANO9-HEK cells began to develop 5 s to a few minutes after the formation of whole cells. This time lag suggests a possible indirect signaling pathway for the activation by cAMP.

Cholera toxin is an oligomeric protein complex secreted by the bacterium *Vibrio cholerae* that leads to the direct activation of adenylyl cyclase, resulting in the overproduction of cAMP [40]. If ANO9 is activated by cAMP and its downstream signal, then the application of cholera toxin should activate ANO9. Indeed, the application of cholera toxin to the bath solution evoked robust currents with variable time lags in ANO9-HEK cells. However, the cholera toxin-induced currents were not observed in the mock-transfected HEK293T cells (Fig. 1E and F).

3.2. PKA activates ANO9

We then tested whether cAMP alone or with its downstream signal, PKA, activated ANO9. To do this, membrane patches were isolated from ANO9-HEK cells with an inside-out patch configuration. Recordings were made in a pipette solution containing 140 mM NaCl and 2 mM $CaCl_2$ and a bath solution containing 140 mM KCl at E_{hold} = −60 mV. When solutions containing 100 μM cAMP, 2 mM ATP or cAMP + ATP were applied to the inside-out patches, no appreciable currents were observed (Fig. 2A). However, when recombinant catalytic subunit of PKA (2500 units/ml) together with 2 mM ATP was applied to isolated membrane patches of ANO9-HEK cells, large macroscopic currents were observed (Fig. 2A**)**. These currents were also observed at depolarization potential (E_{hold} = +30 mV). These results now suggest that the phosphorylation by PKA is necessary for the activation of ANO9. Therefore, we determined if PKA can phosphorylate ANO9. To do this, the lysates of HA-ANO9-HEK cells was precipitated with the anti-HA antibodies. The immunoprecipitants were treated with the recombinant catalytic subunit of PKA and ATP. Then we immunoblotted the precipitants with anti-phosphoserine antibodies. As shown in Fig. 2C, anti-phosphoserine antibodies detect ANO9 proteins in PKA treated HA-immunoprecipitates. The protein band was not detected in HA-immunoprecipitates that were not treated with PKA. Thus, these results suggest that ANO9 is activated by phosphorylation by PKA.

3.3. ANO9 is a cation channel

The cAMP-evoked currents in ANO9-HEK cells were cationic because they were not observed in the bath solution containing 140 mM *N*-methyl D-glucamine (NMDG)-Cl (Fig. 3A and B). Ion selectivity was determined by a shift in reversal potential in whole cells in which extracellular KCl solution was changed to 70 and 210 mM. The pipette solution contained 140 mM KCl. The current–voltage (I–V) relationship was obtained to measure the reversal potential. Voltage ramps from −100 mV to +100 mV in 100 ms durations were applied. When the bath KCl concentration, initially 140 mM, was changed to 210 mM and 70 mM, the reversal potentials were changed to +6.29 ± 0.82 mV and −11.46 ± 1.09 mV (n = 8), respectively (Fig. 3C). The reversal potentials were plotted as a function of extracellular KCl concentration on a semi-logarithmic scale. A line was fitted to +37.2 mV/decade, which is relatively close to +58 mV/decade of the Nernst equation when the major carrier charge is a cation. The relative permeability ratio of K^+ and Cl^- (P_{Cl}/P_{K}) calculated by Goldman-Hodgkin-Katz equation [41] is 0.237 ± 0.034, suggesting a weak permeability to Cl^-. Thus, these results clearly suggest that ANO9 exhibits a large preference for cations.

We then explored the selectivity among cations by estimating the permeability ratios after replacing the 140 mM KCl solution in the bath with a solution of 70 mM $CaCl_2$ and 140 mM of NaCl, CsCl, and LiCl. The pipette solution contained 140 mM KCl. The reversal potentials were −2.07 ± 1.56, −7.83 ± 1.25, −1.06 ± 2.43 and −12.6 ± 2.96 mV when the bath K^+ solution was changed to Ca^{2+}, Cs^+, Na^+, and Li^+, respectively (Fig. 3D). The relative permeability ratios (P_X/P_K) ranged from 0.54 to 1.87 (Fig. 3E), suggesting that ANO9 discriminated poorly among cations but was more permeable to Ca^{2+} than to monovalent cations.

Because both ANO1 and ANO2 are known to be voltage-activated [42,43], we investigated if ANO9 was also activated by voltage alone. We applied the voltage steps from −100 mV to 100 mV in 10 mV increment to the whole cells of mock- and *Ano9*-transfected HEK cells. The whole-cells were treated with a K_v blocker, 4-aminopyridine to block voltage-gated K^+ channels in HEK cells. Shown in Fig. 3G, *Ano9*-transfected cells showed the comparable shape and reversal potential of the I–V curve to those of mock-transfected cells, suggesting that voltage alone not activate ANO9.

3.4. Calcium influx through ANO9 induced by cAMP

The activation of ANO9 by intracellular cAMP was also determined by calcium imaging experiments. ANO9-expressing cells displayed irregular calcium signals after the treatment with 2 mM N^6,2′-O-dibutyryladenosine 3′,5′-cyclic monophosphate (db-cAMP), a cell-permeable form of cAMP. The db-cAMP-induced Ca^{2+} transients were blocked by the pretreatment with H-89 (Fig. 4A and B). The db-cAMP-evoked calcium transients were not detected in the mock-transfected HEK cells (Fig. 4A and B)

3.5. Calcium augments the cAMP-induced ANO9 currents

Because ANO1 and ANO2 are known to be activated by intracellular Ca^{2+}, we also tested for the activation of ANO9 by Ca^{2+}. When 1 μM Ca^{2+} was applied to the pipette, no appreciable whole-cell currents were activated. When 10 μM Ca^{2+} was applied, small currents were observed (Fig. 5B and C). When 20 μM cAMP was applied together with

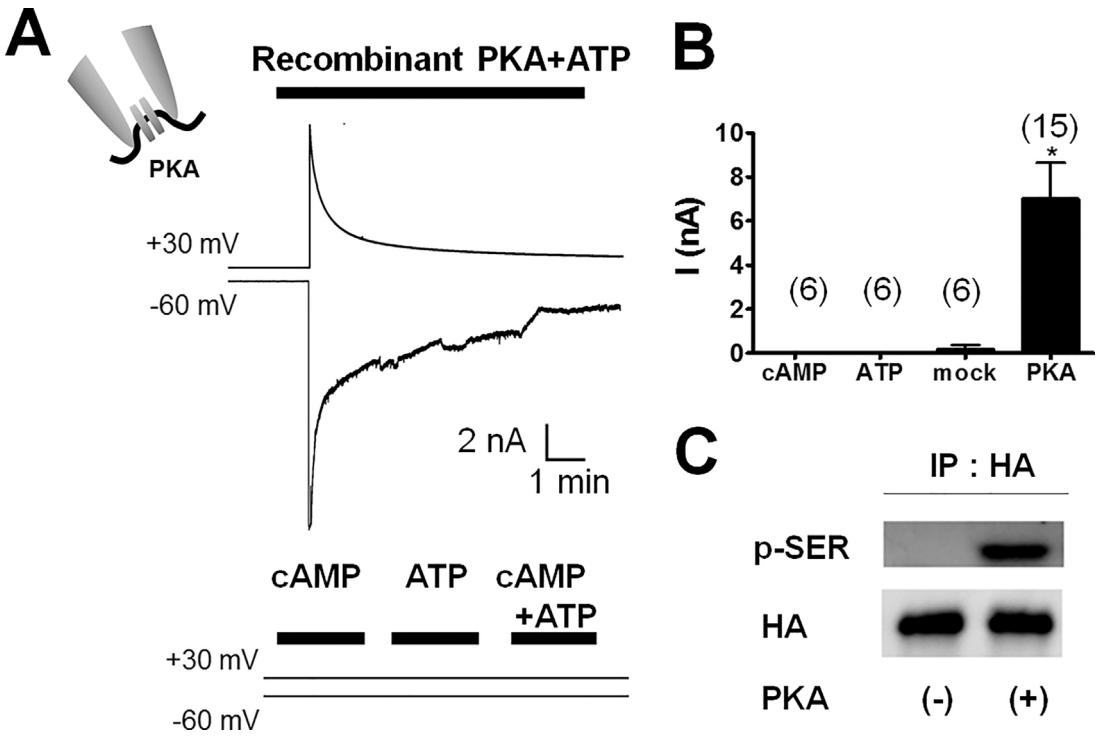

Fig. 2. The phosphorylation by PKA activates ANO9.
(A) Representative traces of macroscopic currents of inside-out membrane patches from ANO9-HEK cells. The application of recombinant catalytic subunit of PKA (2500 units/ml) with 2 mM ATP to the bath evoked robust currents (upper) whereas the application of cAMP and ATP alone failed to evoke the macroscopic currents (lower).
(B) Summary of the PKA-evoked currents in ANO9-HEK cells in inside-out patch configuration.
(C) Phosphorylation of ANO9 at Ser residues by PKA. The lysates of HA-ANO9-HEK cells were precipitated with anti-HA antibodies. The immunoprecipitates were treated with recombinant catalytic subunit of PKA followed by blotting with anti-phosphoserine antibodies.

10 μM Ca^{2+}, much larger currents than those activated by 10 μM Ca^{2+} alone were observed. These current responses to the co-application of Ca^{2+} and cAMP appeared to be dose dependent because larger currents were observed when 100 and 200 μM cAMP were applied along with 10 μM Ca^{2+} (Fig. 5B and C). Although the intracellular Ca^{2+} in a physiological concentration rarely activated ANO9, Ca^{2+} can augment the ANO9 response to cAMP.

3.6. Intracellular sodium inhibits ANO9

Unexpectedly, we also found that a high intracellular concentration of Na^+ inhibits the activity of ANO9. Intracellular cAMP vigorously activated ANO9 when 0 mM Na^+ was added to the pipette (intracellular) solution. However, when 50 mM NaCl was added to the pipette solution, the cAMP-evoked whole-cell currents were markedly reduced (Fig. 6A and B). In contrast, when 50 mM CsCl was added to the pipette solution, the cAMP-evoked currents were comparable to those of the pipette solution containing 150 mM KCl (Fig. 6A and B). These results suggest that high intracellular concentration of Na^+ inhibited the cAMP-dependent ANO9 activity.

3.7. Ano9 is rich in intestines

Tissue distribution of *Ano9* was determined. *Ano9* mRNAs were mainly observed in the digestive system. The small intestine, colon, and stomach expressed a large number of copies of *Ano9* mRNA. A small amount of *Ano9* mRNA was also detected in the tongue, kidney, eye, lung, and bladder (Fig. 7A). Consistent with high expression in the colon, ANO9 is known to be expressed in colorectal cancer cells (SW480) [37]. Indeed, the ANO9 specific immunofluorescence was present in the plasma membrane of SW480 cells when probed with anti-ANO9 antibodies (Fig. 7B). In SW480 cells, phosphorylated ANO9 at Ser residues was detected when the immunoprecipitates were treated with recombinant catalytic subunit of PKA but not in PKA non-treated immunoprecipitates (Fig. 7C).

We therefore determined if cAMP activated the cation currents in these cells. Shown in Fig. 7D, the intracellular application of 100 μM cAMP resulted in large inward currents in 15 out of 20 SW480 cells. The cAMP-evoked currents were blocked by co-challenge with 20 μM H-89 in the pipette solution. In addition, a knock-down of *Ano9* in the SW480 cells after transfection with siRNA of *Ano9* markedly reduced the cAMP-evoked currents (Fig. 7D and E). These results demonstrate that the native ANO9 in colorectal cells is activated by intracellular cAMP.

4. Discussion

4.1. Diverse functions of the anoctamin family

The anoctamins have 10 homologs with diverse cellular and physiological functions. ANO1 was first discovered as a calcium-activated chloride channel [1,3] and is known to be involved in many physiological functions such as fluid secretion, smooth muscle contraction, nociception, tumorigenesis and cell proliferation [4–9,15,44]. ANO2 is also known to be a calcium-activated chloride channel with olfaction and learning and memory functions [18,20,23,24,45]. ANO3 is known to increase modulation of the activity of the Na^+-activated K^+ channel in dorsal-root ganglion neurons, and it also modulates nociception [46]. ANO5, expressed in muscles and bones, has been implicated in skeletomuscular functions because its mutations cause a skeletomuscular disease, gnathodiaphyseal dysplasia [34]. Despite their physiological implications, however, the activation mechanisms and other cellular functions of ANO3 and ANO5 are not well characterized. ANO6 was initially characterized as a scramblase that disrupted polarized phospholipids in the plasma membrane [31,32]. Later, ANO6 was found to be a cation channel activated by Ca^{2+} [27]. Despite the diverse functions of anoctamins, the activation mechanisms of those other than

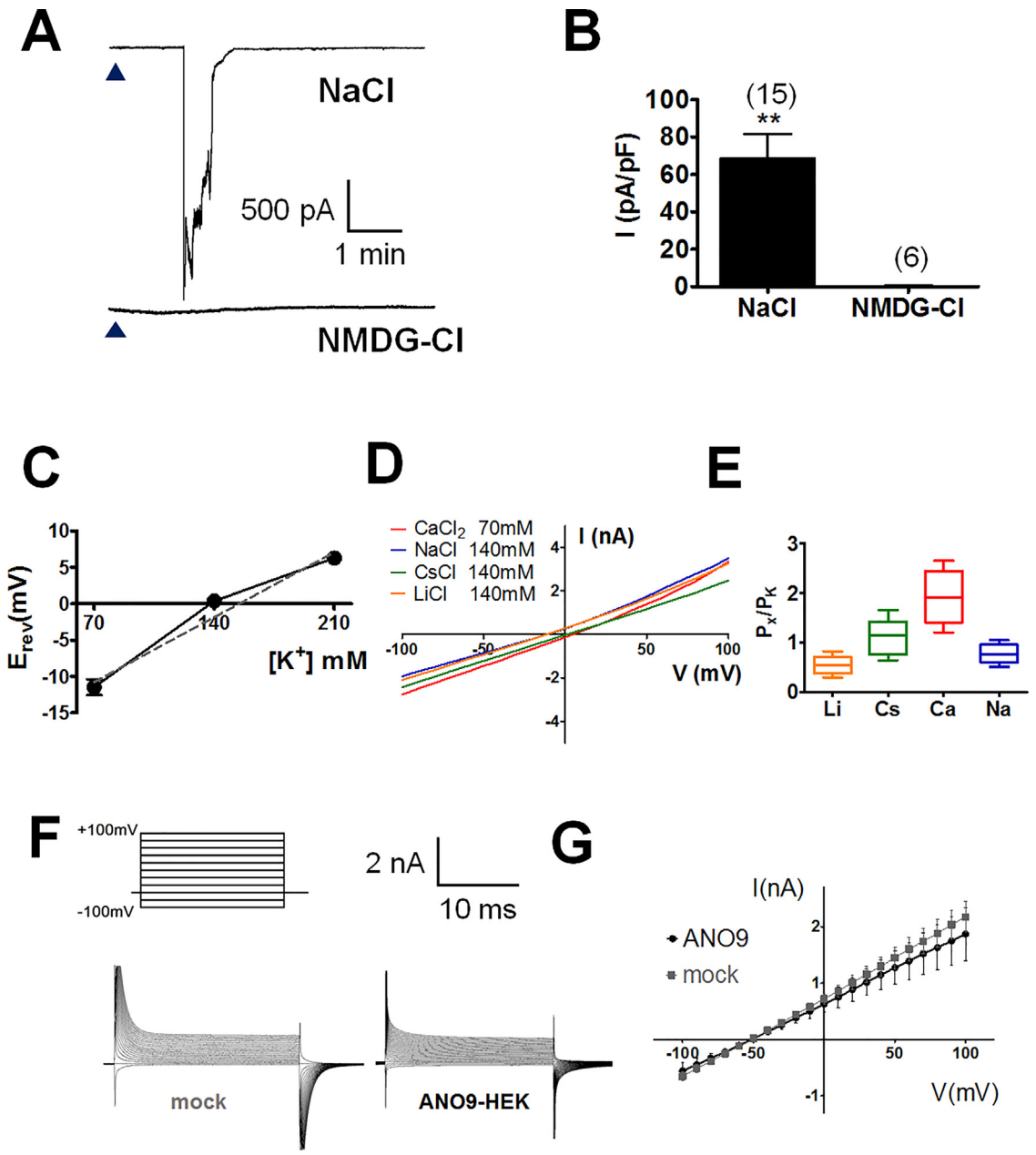

Fig. 3. ANO9 is a cation channel.

(A) Whole-cell currents of ANO9-HEK cells activated by 100 μM cAMP in 140 mM NaCl (upper) but not in 140 mM NMDG-Cl (lower) bath solutions.

(B) The average current densities of ANO9-HEK cells activated by the intracellular cAMP at NaCl or NMDG-Cl solution condition.

(C) Reversal potentials in different KCl concentration gradients between pipette and bath solutions. Reversal potentials were measured under bi-ionic conditions where the pipette contained 140 mM KCl whereas the bath contained 70, 140 or 210 mM KCl. The permeability ratios, P_X/P_K was calculated using the Goldman-Hodgkin-Katz equation.

(D-E) Cation selectivity of cAMP-induced ANO9 currents. Representative I–V curves (D) and the permeability ratios (P_X/P_K) (E) of ANO9 currents. Whole cells were formed with the pipette contained 140 mM KCl. Current-voltage relationship were obtained after the bath solution was changed to 70 mM $CaCl_2$, 140 mM NaCl, 140 mM CsCl, and 140 mM LiCl. The permeability ratios, P_X/P_K was calculated using the Goldman-Hodgkin-Katz equation.

(F-G) Whole-cell currents (F) and the I–V curves of ANO9-HEK cells elicited by voltage steps. Voltage steps from −100 to +100 mV in 10 mV increment were applied to whole cells of HEK cells transfected with vector alone (mock) or Ano9 (ANO9-HEK). The bath solution of whole cells contained the K_v inhibitor, 4-aminopyridine.

ANO1, ANO2 and ANO6 are not well understood.

Unlike ANO1 and ANO2, ANO9 was permeated mainly by cations. The ANO9 currents were not blocked by the ANO1 blockers such as MONNA, NPPB, or tannic acid (Fig. 1B and C). More importantly, ANO9 was activated by the cAMP/PKA pathway but not by Ca^{2+} or voltage. Although ANO9 is known to be expressed in the intestines, its physiological function is largely unknown. However, if ANO9 is expressed in the epithelium of the intestines, its role in controlling fluid secretion or absorption may be expected. Precise role of ANO9 in the intestines needs to be clarified in future.

4.2. Role in tumorigenesis

ANO9 has been implicated in intestinal functions; notably, its transcription levels were much higher in intestines compared to other tissues (Fig. 7A; [47,48]). It is expressed in the colorectal cancer cell line, SW480 cells. We observed cAMP-activated and H-89-reversible currents in the SW480 cells (Fig. 7D), and ANO9 has been linked to colorectal cancer [37,38]. Li et al. found that the activity of ANO9 was negatively associated with tumorigenesis in the colon [37]. The expression of ANO9 was higher in non-tumor tissue than in tumorous

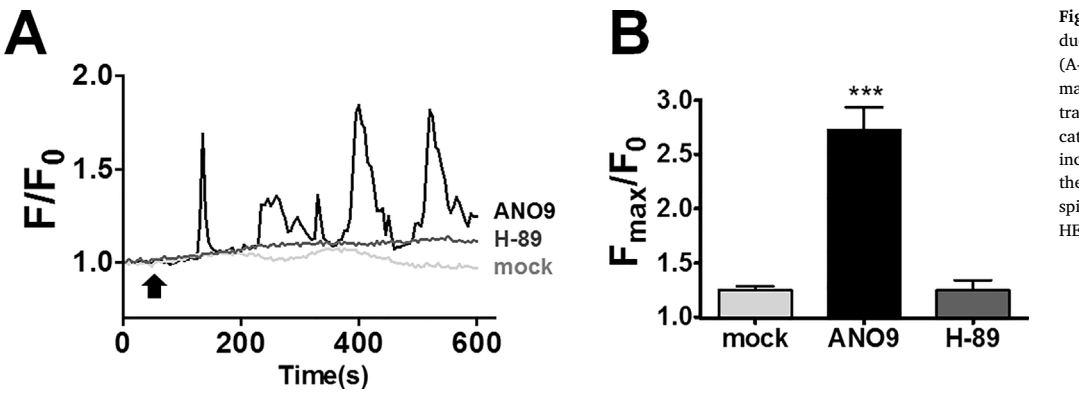

Fig. 4. Calcium influx through ANO9 induced by cAMP.
(A-B) Representative traces (A) and summary (B) of Ca^{2+} spikes of ANO9- or mock-transfected HEK293T cells after the application (arrow) of 2 mM dbcAMP. Cells were incubated with 1 μM Fluo3-AM. Note that the application of dbcAMP evoked Ca^{2+} spikes in ANO9-HEK cells but not in mock-HEK or H-89-pretreated ANO9-HEK cells.

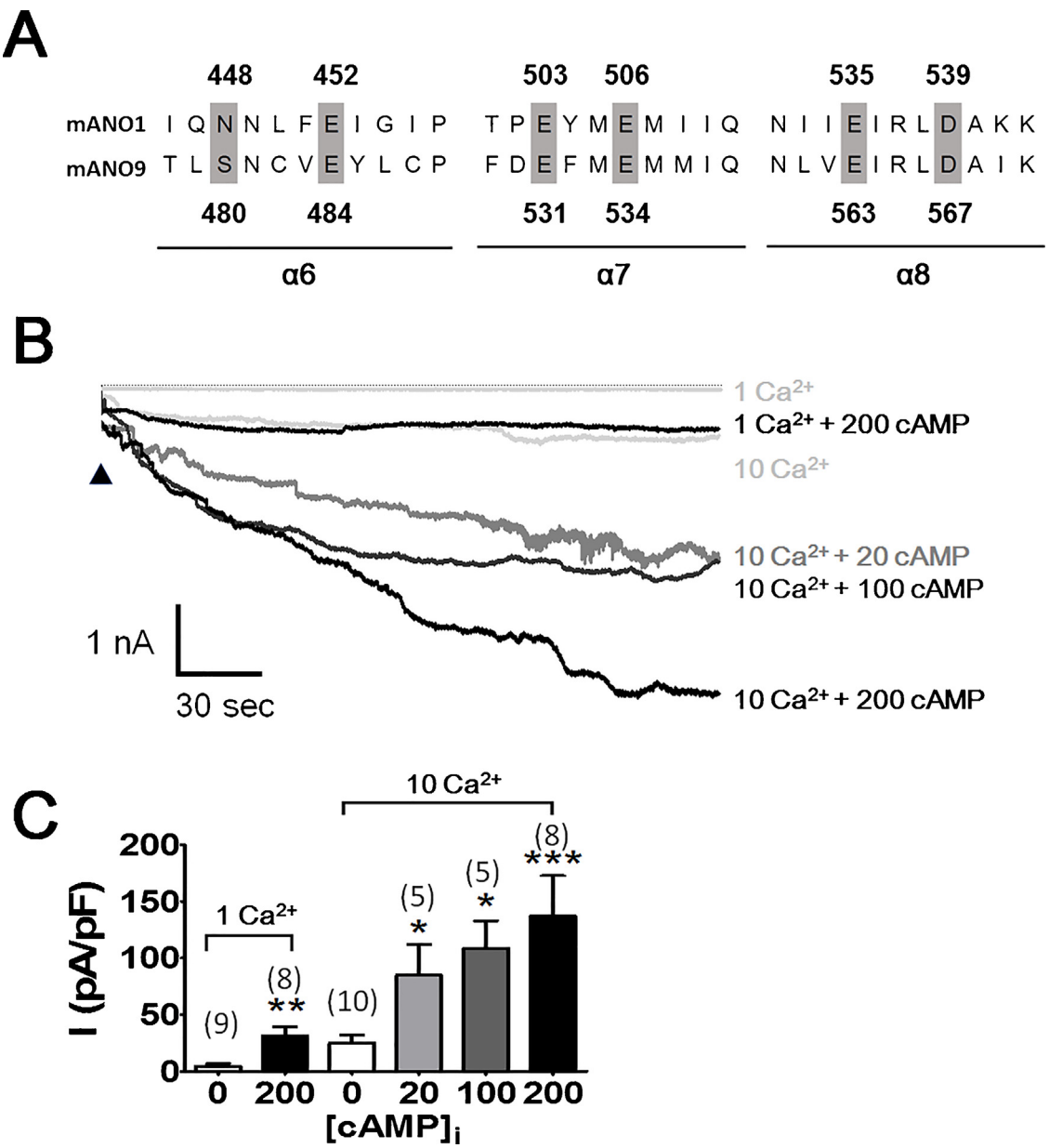

Fig. 5. Intracellular calcium augments the cAMP-induced ANO9 activity.
(A) Sequence alignment with mouse ANO1 and mouse ANO9 at the putative Ca^{2+} binding sites in ANO1. The conserved amino acids in the putative Ca^{2+} binding sites are highlighted in gray.
(B) Whole-cell currents ANO9-HEK cells activated by various concentrations of intracellular cAMP or/and Ca^{2+}. The bath and pipette solutions are same as in Fig. 1.
(C) Summary of the cAMP-induced currents at 1 or 10 μM Ca^{2+}.* $p < 0.05$, ** $p < 0.01$, *** $p < 0.001$, one way of ANOVA, Tukey's post-hoc test.

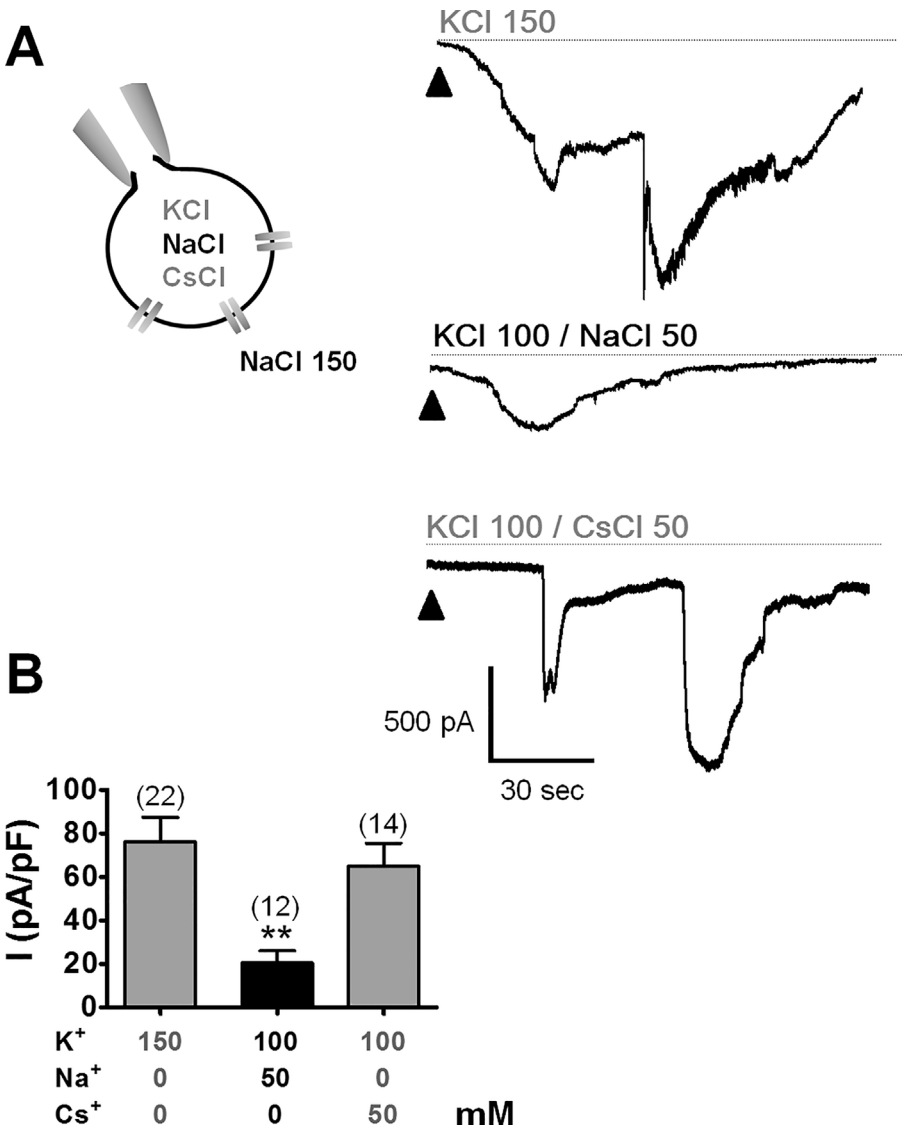

Fig. 6. Intracellular sodium inhibits ANO9.
(A) cAMP-induced whole-cell currents of ANO9-HEK cells with or without intracellular Na^+. Concentration of KCl, NaCl or CsCl in the pipette solution was shown in each trace. The bath solution contained 150 mM NaCl.
(B) Summary of cAMP-induced currents with different pipette solutions. ** $p < 0.01$, one way of ANOVA, Tukey's post-hoc test.

tissues. ANO9 expression was lower in the recurrent colorectal cancer cells than in non-recurrent colorectal cancer cells. ANO9 overexpression is known to reduce the invasion of cancer cells [37]. Lower levels of ANO9 expression have been associated with poorer prognoses in patients with higher expression levels [37]. On the contrary, in the pancreas, ANO9 appears to promote cancer [38]. Jun et al. reported that ANO9 is rarely expressed in normal pancreas, as also observed in this study (Fig. 7A) [38]. However, the ANO9 expression is increased in pancreatic cancer cell lines. Overexpression of ANO9 promotes cell proliferation in cell cultures. Knockdown of ANO9 inhibits cell proliferation. More importantly, the ANO9 expression is a poor prognostic factor in pancreatic cancer patients [38]. There is no plausible explanation regarding the discrepancy in two cases. Maybe tissue difference such as colon and pancreas may account for the different results. Although a clear explanation is lacking, it seems clear that ANO9 plays a role in regulating tumorgenesis in the intestines and pancreas.

4.3. Calcium dependence

Ca^{2+} is indispensable for anoctamin functions, and it activates ANO1 and ANO2 [1–3,20]. Ca^{2+} is also required for the scramblase activity of ANO6 and fungal TMEM16 [27,32,33]. However, Ca^{2+} was not found to be essential for the activation of ANO9 because physiological concentrations of Ca^{2+} rarely gated ANO9. Also, cAMP activated ANO9 in Ca^{2+}-free conditions. However, Ca^{2+} augmented the cAMP-induced ANO9 currents. In addition, the kinetics of gating is also changed by the addition of Ca^{2+}. ANO9 activation by cAMP in Ca^{2+} free condition needs time lag after making whole-cells. In contrast, with high intracellular [Ca^{2+}], cAMP activated the channel almost immediately after the formation of whole-cells. In addition, the rate of activation by cAMP is also changed when Ca^{2+} is added. For example, without Ca^{2+}, cAMP abruptly activated the channel (Figs. 1B and 3A). However, when high Ca^{2+} is added, cAMP slowly activated the channel (Fig. 5B). Thus, the role of Ca^{2+} in activating ANO9 cannot be ignored because Ca^{2+} affected the ANO9 activity. Recently, the X-ray crystal structure of nhTMEM16 was determined [49]. The Glu residues of ANO1 essential for its activation by Ca^{2+} were located in the subunit cavity of ANO1 in the hydrophobic core of the membrane. The subunit cavity was lined with four glutamates, an aspartate and an asparagine residue in the α-helices 6, 7, and 8 of ANO1. These helices are known to be crucial for the channel activation of ANO1 and the scramblase activity of nhTMEM16 [49]. ANO9 has a similar amino-acid sequence in this region (Fig. 5A): ANO9 has four glutamates, an aspartate and a serine residue in the α-helices 6, 7 and 8. This structural constraint of ANO9 compared to ANO1 predicts the synergistic but not essential role of Ca^{2+} in activating ANO9. Voltage has been found to be another endogenous activator of ANO1 and ANO2, but, analogous to the role of Ca^{2+}, ANO9 was not activated by voltage alone (Fig. 3F and

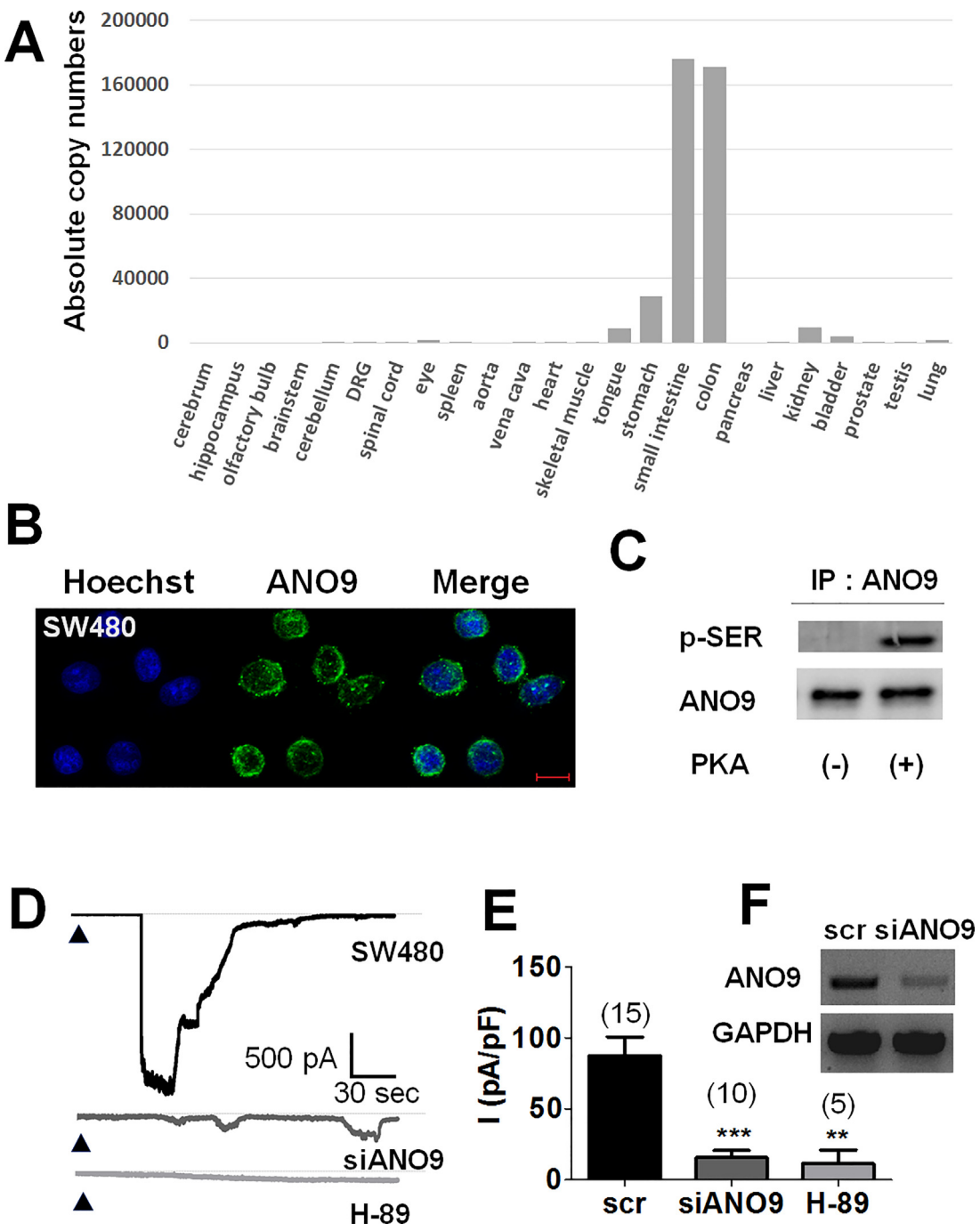

Fig. 7. ANO9 is highly expressed in colonic cells.
(A) Real-time quantitative PCR analysis of mRNA transcripts encoding ANO9 in various mouse organs. The levels of transcripts were expressed as absolute copy numbers.
(B) The immunofluorescence of ANO9 in SW480 cells. Scale bar = 10 μm.
(C) Phosphorylation of endogenous ANO9 by PKA. The lysates of SW480 cells were precipitated with anti-ANO9 antibodies. The immunoprecipitates were treated with recombinant catalytic subunit of PKA followed by blotting with anti-phosphoserine antibodies.
(D) Whole-cell currents activated by intracellular cAMP (100 μM) with (upper) or without *Ano9* siRNA treatment (middle). The currents were also blocked by the H-89 pretreatment (lower).
(E) Summary of the cAMP-induced currents in the SW480 cells. scr; scrambled siRNA treated, siRNA; Ano9 siRNA treated; H-89, H-89 treated.
(F) Real-time quantitative PCR products of Ano9 in SW480 cells transfected with scrambled or Ano9 siRNAs. PCR products of glyceraldehyde-3-phosphate dehydrogenase (GAPDH) mRNAs were also shown for control.

G). We found that ANO9 added more to the diversity of the functions of the anoctamin family.

4.4. PKA activation

Many of the functions of the cystic fibrosis transmembrane conductance regulator (CFTR), such as the transepithelial Cl^- transport in various epithelia, overlap with those of ANO1 mainly because they are both anion channels. Because of this functional overlap, ANO1 has been considered to rescue the defective CFTR functions in cystic fibrosis [50,51]. CFTR is activated by ATP and PKA and has multiple trans-membrane-spanning domains in the cell membrane and a regulatory

domain and two nucleotide-binding domains in the cytosolic side [52]. The binding of ATP to the nucleotide-binding domains is known to activate the CFTR while the phosphorylation of the regulatory domain by PKA is a prerequisite for the activation. Unlike the CFTR, ANO9 does not contain nucleotide-binding domains, and therefore ANO9 gating does not require ATP because it is not activated by ATP alone (Fig. 2B). However, ANO9 is activated by the direct application of catalytic subunit of PKA. In addition, PKA inhibitors blocked the cAMP-induced ANO9 currents. Thus, it is highly likely that ANO9 opens only when it is phosphorylated by PKA. Consistent with this, the phosphorylation on serine residues in ANO9 is confirmed by in vitro kinase assay (Figs. 2C and 7C).

ANO9 currents activated by cAMP or PKA inactivated rapidly. This inactivation is observed in the presence of phosphatase inhibitor cocktails in the pipette solution, suggesting that the inactivation appears independent on dephosphorylation (data not shown). In addition, the inactivation of ANO9 currents persists at the depolarization (Fig. 2A). Thus, the inactivation is independent on membrane potentials.

4.5. Inhibition by intracellular Na^+

In the present study, we observed that intracellular Na^+ inhibits ANO9. However, the meaning of the inhibition by Na^+ is unclear. Intracellular Na^+ inhibits intracellular Ca^{2+} via the activity of Na^+/Ca^{2+} exchangers. In this context, intracellular Na^+ inhibits ANO9 to block the Ca^{2+} influx via ANO9. However, more plausible explanation awaits for future studies.

Conflict of interest

The authors declare no conflict of interests to any institution or company.

Acknowledgements

This study was supported by the National Research Foundation of Korea, funded by the Ministry of Science and ICT (2011-0018358).

References

[1] A. Caputo, E. Caci, L. Ferrera, N. Pedemonte, C. Barsanti, E. Sondo, et al., TMEM16A, a membrane protein associated with calcium-dependent chloride channel activity, Science 322 (2008) 590–594.
[2] B.C. Schroeder, T. Cheng, Y.N. Jan, L.Y. Jan, Expression cloning of TMEM16A as a calcium-activated chloride channel subunit, Cell 134 (2008) 1019–1029.
[3] Y.D. Yang, H. Cho, J.Y. Koo, M.H. Tak, Y. Cho, W.S. Shim, et al., TMEM16A confers receptor-activated calcium-dependent chloride conductance, Nature 455 (2008) 1210–1215.
[4] F. Huang, H. Zhang, M. Wu, H. Yang, M. Kudo, C.J. Peters, et al., Calcium-activated chloride channel TMEM16A modulates mucin secretion and airway smooth muscle contraction, Proc. Natl. Acad. Sci. U. S. A. 109 (2012) 16354–16359.
[5] Y. Jang, U. Oh, Anoctamin 1 in secretory epithelia, Cell Calcium 55 (2014) 355.
[6] W. Namkung, P.W. Phuan, A.S. Verkman, TMEM16A inhibitors reveal TMEM16A as a minor component of calcium-activated chloride channel conductance in airway and intestinal epithelial cells, J. Biol. Chem. 286 (2011) 2365–2374.
[7] J. Ousingsawat, J.R. Martins, R. Schreiber, J.R. Rock, B.D. Harfe, K. Kunzelmann, Loss of TMEM16A causes a defect in epithelial Ca^{2+}-dependent chloride transport, J. Biol. Chem. 284 (2009) 28698–28703.
[8] V.G. Romanenko, M.A. Catalan, D.A. Brown, I. Putzier, H.C. Hartzell, A.D. Marmorstein, et al., Tmem16A encodes the Ca^{2+}-activated Cl^- channel in mouse submandibular salivary gland acinar cells, J. Biol. Chem. 285 (2010) 12990–13001.
[9] H. Cho, Y.D. Yang, J. Lee, B. Lee, T. Kim, Y. Jang, et al., The calcium-activated chloride channel anoctamin 1 acts as a heat sensor in nociceptive neurons, Nat. Neurosci. 15 (2012) 1015–1021.
[10] S. Bulley, Z.P. Neeb, S.K. Burris, J.P. Bannister, C.M. Thomas-Gatewood, W. Jangsangthong, et al., TMEM16A/ANO1 channels contribute to the myogenic response in cerebral arteries, Circ. Res. 111 (2012) 1027–1036.
[11] S.J. Hwang, P.J. Blair, F.C. Britton, K.E. O'Driscoll, G. Hennig, Y.R. Bayguinov, et al., Expression of anoctamin 1/TMEM16A by interstitial cells of Cajal is fundamental for slow wave activity in gastrointestinal muscles, J. Physiol. 587 (2009) 4887–4904.
[12] C.A. Cobine, E.E. Hannah, M.H. Zhu, H.E. Lyle, J.R. Rock, K.M. Sanders, et al., ANO1 in intramuscular interstitial cells of Cajal plays a key role in the generation of slow waves and tone in the internal anal sphincter, J. Physiol. 595 (2017) 2021–2041.
[13] A. Britschgi, A. Bill, H. Brinkhaus, C. Rothwell, I. Clay, S. Duss, et al., Calcium-activated chloride channel ANO1 promotes breast cancer progression by activating EGFR and CAMK signaling, Proc. Natl. Acad. Sci. U. S. A. 110 (2013) E1026–E1034.
[14] L. Jia, W. Liu, L. Guan, M. Lu, K. Wang, Inhibition of calcium-activated chloride channel ANO1/TMEM16A suppresses tumor growth and invasion in human lung cancer, PLoS One 10 (2015) e0136584.
[15] U. Duvvuri, D.J. Shiwarski, D. Xiao, C. Bertrand, X. Huang, R.S. Edinger, et al., TMEM16A induces MAPK and contributes directly to tumorigenesis and cancer progression, Cancer Res. 72 (2012) 3270–3281.
[16] J.Y. Cha, J. Wee, J. Jung, Y. Jang, B. Lee, G.S. Hong, et al., Anoctamin 1 (TMEM16A) is essential for testosterone-induced prostate hyperplasia, Proc. Natl. Acad. Sci. U. S. A. 112 (2015) 9722–9727.
[17] S. Pifferi, M. Dibattista, A. Menini, TMEM16B induces chloride currents activated by calcium in mammalian cells, Pflugers Arch. 458 (2009) 1023–1038.
[18] W.C. Huang, S. Xiao, F. Huang, B.D. Harfe, Y.N. Jan, L.Y. Jan, Calcium-activated chloride channels (CaCCs) regulate action potential and synaptic response in hippocampal neurons, Neuron 74 (2012) 179–192.
[19] W. Zhang, S. Schmelzeisen, D. Parthier, S. Frings, F. Mohrlen, Anoctamin calcium-activated chloride channels may modulate inhibitory transmission in the cerebellar cortex, PLoS One 10 (2015) e0142160.
[20] A.B. Stephan, E.Y. Shum, S. Hirsh, K.D. Cygnar, J. Reisert, H. Zhao, ANO2 is the cilial calcium-activated chloride channel that may mediate olfactory amplification, Proc. Natl. Acad. Sci. U. S. A. 106 (2009) 11776–11781.
[21] K. Dauner, C. Mobus, S. Frings, F. Mohrlen, Targeted expression of anoctamin calcium-activated chloride channels in rod photoreceptor terminals of the rodent retina, Invest. Ophthalmol. Vis. Sci. 54 (2013) 3126–3136.
[22] S. Keckeis, N. Reichhart, C. Roubeix, O. Strauss, Anoctamin2 (TMEM16B) forms the Ca^{2+}-activated Cl^- channel in the retinal pigment epithelium, Exp. Eye Res. 154 (2017) 139–150.
[23] G.M. Billig, B. Pal, P. Fidzinski, T.J. Jentsch, Ca^{2+}-activated Cl^- currents are dispensable for olfaction, Nat. Neurosci. 14 (2011) 763–769.
[24] G. Pietra, M. Dibattista, The Ca^{2+}-activated Cl^- channel TMEM16B regulates action potential firing and axonal targeting in olfactory sensory neurons, J. Gen. Physiol. 148 (2016) 293–311.
[25] A.S. Forrest, J.E. Angermann, R. Raghunathan, C. Lachendro, I.A. Greenwood, N. Leblanc, Intricate interaction between store-operated calcium entry and calcium-activated chloride channels in pulmonary artery smooth muscle cells, Adv. Exp. Med. Biol. 661 (2010) 31–55.
[26] K. Bernstein, J.Y. Vink, X.W. Fu, H. Wakita, J. Danielsson, R. Wapner, et al., Calcium-activated chloride channels anoctamin 1 and 2 promote murine uterine smooth muscle contractility, Am. J. Obstet. Gynecol. 211 (688) (2014) e681–610.
[27] H. Yang, A. Kim, T. David, D. Palmer, T. Jin, J. Tien, et al., TMEM16F forms a Ca^{2+}-activated cation channel required for lipid scrambling in platelets during blood coagulation, Cell 151 (2012) 111–122.
[28] Y. Hu, J.H. Kim, K. He, Q. Wan, J. Kim, M. Flach, Scramblase TMEM16F terminates T cell receptor signaling to restrict T cell exhaustion, J. Exp. Med. 213 (2016) 2759–2772.
[29] C. Xu, E. Gagnon, M.E. Call, J.R. Schnell, C.D. Schwieters, C.V. Carman, et al., Regulation of T cell receptor activation by dynamic membrane binding of the CD3 epsilon cytoplasmic tyrosine-based motif, Cell 135 (2008) 702–713.
[30] H. Zhang, S.P. Cordoba, O. Dushek, P.A. van der Merwe, Basic residues in the T-cell receptor zeta cytoplasmic domain mediate membrane association and modulate signaling, Proc. Natl. Acad. Sci. U. S. A. 108 (2011) 19323–19328.
[31] E. Castoldi, P.W. Collins, P.L. Williamson, E.M. Bevers, Compound heterozygosity for 2 novel TMEM16F mutations in a patient with Scott syndrome, Blood 117 (2011) 4399–4400.
[32] J. Suzuki, M. Umeda, P.J. Sims, S. Nagata, Calcium-dependent phospholipid scrambling by TMEM16F, Nature 468 (2010) 834–838.
[33] M. Malvezzi, M. Chalat, R. Janjusevic, A. Picollo, H. Terashima, A.K. Menon, et al., Ca^{2+}-dependent phospholipid scrambling by a reconstituted TMEM16 ion channel, Nat. Commun. 4 (2013) 2367.
[34] T.T. Tran, K. Tobiume, C. Hirono, S. Fujimoto, K. Mizuta, K. Kubozono, et al., TMEM16E (GDD1) exhibits protein instability and distinct characteristics in chloride channel/pore forming ability, J. Cell. Physiol. 229 (2014) 181–190.
[35] A. Picollo, M. Malvezzi, A. Accardi, TMEM16 proteins: unknown structure and confusing functions, J. Mol. Biol. 427 (2015) 94–105.
[36] J.R. Rock, B.D. Harfe, Expression of TMEM16 paralogs during murine embryogenesis, Dev. Dyn. 237 (2008) 2566–2574.
[37] C. Li, S. Cai, X. Wang, Z. Jiang, Identification and characterization of ANO9 in stage II and III colorectal carcinoma, Oncotarget 6 (2015) 29324–29334.
[38] I. Jun, H.S. Park, H. Piao, J.W. Han, M.J. An, B.G. Yun, et al., ANO9/TMEM16J promotes tumourigenesis via EGFR and is a novel therapeutic target for pancreatic cancer, Br. J. Cancer 117 (12) (2017) 1798–1809.
[39] J. Lee, J. Jung, M.H. Tak, J. Wee, B. Lee, Y. Jang, et al., Two helices in the third intracellular loop determine anoctamin 1 (TMEM16A) activation by calcium, Pflugers Arch. 467 (2015) 1677–1687.
[40] S.E. Gabriel, K.N. Brigman, B.H. Koller, R.C. Boucher, M.J. Stutts, Cystic fibrosis heterozygote resistance to cholera toxin in the cystic fibrosis mouse model, Science 266 (1994) 107–109.
[41] B. Hille, Selective permeability: independence, in: B. Hille (Ed.), Ion Channels of Excitable Membranes, 3rd ed., Sinauer Associate, Sunderland, 2001, pp. 441–470.
[42] Q. Xiao, K. Yu, P. Perez-Cornejo, Y. Cui, J. Arreola, H.C. Hartzell, Voltage- and

calcium-dependent gating of TMEM16A/Ano1 chloride channels are physically coupled by the first intracellular loop, Proc. Natl. Acad. Sci. U. S. A. 108 (2011) 8891–8896.
[43] V. Cenedese, G. Betto, F. Celsi, O.L. Cherian, S. Pifferi, A. Menini, The voltage dependence of the TMEM16B/anoctamin2 calcium-activated chloride channel is modified by mutations in the first putative intracellular loop, J. Gen. Physiol. 139 (2012) 285–294.
[44] M. Katoh, M. Katoh, FLJ10261 gene, located within the CCND1-EMS1 locus on human chromosome 11 q13, encodes the eight-transmembrane protein homologous to C12 orf3, C11orf25 and FLJ34272 gene products, Int. J. Oncol. 22 (2003) 1375–1381.
[45] F. Neureither, K. Ziegler, C. Pitzer, S. Frings, Impaired motor coordination and learning in mice lacking anoctamin 2 calcium-gated chloride channels, Cerebellum (2017) 1–9.
[46] F. Huang, X. Wang, E.M. Ostertag, T. Nuwal, B. Huang, Y.N. Jan, et al., TMEM16C facilitates Na(+)-activated K+ currents in rat sensory neurons and regulates pain processing, Nat. Neurosci. 16 (2013) 1284–1290.
[47] R. Schreiber, I. Uliyakina, P. Kongsuphol, R. Warth, M. Mirza, J.R. Martins, et al., Expression and function of epithelial anoctamins, J. Biol. Chem. 285 (2010) 7838–7845.
[48] R. Schreiber, D. Faria, B.V. Skryabin, P. Wanitchakool, J.R. Rock, K. Kunzelmann, Anoctamins support calcium-dependent chloride secretion by facilitating calcium signaling in adult mouse intestine, Pflugers Arch. 467 (2015) 1203–1213.
[49] J.D. Brunner, N.K. Lim, S. Schenck, A. Duerst, R. Dutzler, X-ray structure of a calcium-activated TMEM16 lipid scramblase, Nature 516 (2014) 207–212.
[50] E. Sondo, E. Caci, L.J. Galietta, The TMEM16A chloride channel as an alternative therapeutic target in cystic fibrosis, Int. J. Biochem. Cell Biol. 52 (2014) 73–76.
[51] F. Becq, M.A. Mall, D.N. Sheppard, M. Conese, O. Zegarra-Moran, Pharmacological therapy for cystic fibrosis: from bench to bedside, J. Cyst. Fibros. 10 (Suppl. 2) (2011) S129–S145.
[52] T.C. Hwang, D.N. Sheppard, Gating of the CFTR Cl^- channel by ATP-driven nucleotide-binding domain dimerisation, J. Physiol. 587 (2009) 2151–2161.